1 **Role of PS synthase in shaping the phospholipidome of *Candida albicans***

2 Chelsi D. Cassilly,[1] Abigail T. Farmer,[2] Anthony E. Montedonico,[1] Terry K. Smith,[3] Shawn R.

3 Campagna,[2] Todd B. Reynolds[1]

4 1. Department of Microbiology, University of Tennessee, Knoxville, TN, USA

5 2. Department of Chemistry, University of Tennessee, Knoxville, TN, USA

6 3. Biomedical Sciences Research Complex, Schools of Biology & Chemistry, , The North Haugh, The

7 University St. Andrews, Fife, KY16 9ST, UK

8

**Abstract**

Phosphatidylserine (PS) synthase (Cho1p) and the PS decarboxylase enzymes (Psd1p and Psd2p), which synthesize PS and phosphatidylethanolamine (PE), respectively, are crucial for *Candida albicans* virulence. Mutations that disrupt these enzymes, which are part of the cytidyldiphosphate-diacylglycerol (CDP-DAG) pathway (*i.e. de novo* pathway), utilised for phospholipid synthesis, compromise virulence. Understanding how losses of PS and/or PE synthesis pathways affect the phospholipidome of *Candida* is important for fully understanding how these enzymes impact virulence. The *cho1*ΔΔ and *psd1*ΔΔ *psd2*ΔΔ mutations cause similar changes in levels of phosphatidic acid (PA), phosphatidylglycerol (PG), phosphatidylinositol (PI), and PS. However, only slight changes were seen in PE and phosphatidylcholine (PC). This finding suggests that the alternative mechanism for making PE and PC, the Kennedy Pathway, can compensate for loss of the *de novo* synthesis pathway. *C. albicans* Cho1p, the lipid biosynthetic enzyme with the most potential as a drug target, has biochemically been characterized, and its substrate specificity and kinetics reveal that these are similar to those previously published for *Saccharomyces cerevisiae* Cho1p.

**Keywords:** lipidomics, phosphatidylserine, phosphatidylethanolamine, phosphatidylglycerol, phosphatidylinositol, phosphatidylcholine,

## Introduction

Fungi of the genus *Candida* are opportunistic pathogens known to cause vulvovaginal, oral, and invasive bloodstream infections in humans. Invasive infections are the most serious, with a mortality rate around 30% (1,2). Currently, there are three main antifungal classes used to treat bloodstream infections of *C. albicans*, the species that causes the majority of these infections (3). These therapies include azoles (e.g. fluconazole), echinocandins (e.g. caspofungin), and polyenes (amphotericin B). Unfortunately, these drugs have limited effectiveness due to documented cases of azole resistance (4), the nephrotoxicity of amphotericin B (5,6), and the requirement for intravenous administration of both amphotericin B and caspofungin. Furthermore, the recent rise in patients that are immunocompromised puts more people at risk every year (7), while also dramatically increasing healthcare costs (4). As a result, it is of utmost importance to find novel antifungals to treat *C. albicans* potently and effectively.

Phospholipids are crucial components of biological membranes in both prokaryotes and eukaryotes. The phospholipidome of *C. albicans* is made up mostly of phosphatidylcholine (PC), phosphatidylethanolamine (PE), phosphatidylserine (PS), phosphatidylinositol (PI), phosphatidylglycerol (PG), and cardiolipin (CL) (8). *C. albicans* has a *de novo* method for producing phospholipids, which involves the conversion of cytidine diphosphate-diacylglycerol (CDP-DAG) into PI, PG, and PS (Fig. 1). Although PI, PG, and PS can be end products; PG and PS can be further modified to form CL and PE, respectively, while PE can subsequently be methylated to produce PC. *C. albicans* also utilizes exogenously provided ethanolamine and choline to produce PE and PC via the Kennedy pathway (9-11).

Previous studies have identified the PS synthase (Cho1p) as a potential drug target in *Candida albicans* (10,12). Studies have been done on the enzymology and lipid profiles associated with PS synthase in *S. cerevisiae* (13), but little characterization of the orthologous enzyme or its effects on lipid profiles in *C. albicans* has been performed. Here we report the phospholipidome of the *Candida albicans* *cho1*Δ/Δ and *psd1*Δ/Δ *psd2*Δ/Δ strains, as well as the enzyme kinetics of *C. albicans* Cho1p, finding both the $K_m$ and $V_{max}$ to be in close agreement with those values reported for *S. cerevisiae* Cho1p (13). The studies described in this report set the stage for further characterization of these enzymes as drug targets.

## Materials and Methods

### Strains used

The SC5314 (wild-type) strain of *C. albicans* and mutants used in this study have been previously described in (10). These include *cho1*ΔΔ (YLC337), *cho1*ΔΔ*::CHO1* (YLC344 ), *psd1*ΔΔ (YLC280), *psd1*ΔΔ*::PSD1* (YLC294), *psd2*ΔΔ (YLC271), *psd2*ΔΔ*::PSD2* (YLC290), *psd1*ΔΔ *psd2*ΔΔ (YLC375). The media used to culture strains was YPD (1% yeast extract, 2% peptone, and 2% dextrose).

### Lipid Isolation for Mass Spectrometric Analysis

Lipid isolations were adapted from the protocol of (14). Cultures were grown overnight, shaking at 30° C in 5 mL of YPD. Cultures were then diluted to 0.4 $OD_{600}$ in 25 mL of YPD and grown for 6 hours, shaking at 30° C. After the 6 hours, cultures were pelleted and washed twice with PBS. The final pellets were incubated for at least 1 hour at -80° C, then lyophilized overnight. Dry mass was then recorded for normalization and pellets were suspended in 500 µL to 1 mL of PBS. The resulting thick suspension was then transferred to Teflon-capped glass tubes (Pyrex) and 1.5 mL of methanol was added. Two scoops of 150-212 µm sized glass beads (Sigma-Aldrich, St. Louis, MO) were added to each tube. Cells were lysed by vigorous vortexing for 30 seconds punctuated by 30 second incubations on ice. 3 mL of chloroform was added and the solution was vortexed briefly before being transferred to 15 mL glass funnel filtration system (Millipore, Billerica, MA, USA) with 24 mm glass microfibre filters (Whatman). Liquid collected was then poured into a separating funnel and washed with 900 µL of sterilize 0.9% NaCl. The mixture was allowed to sit and separate for at least 5 minutes, or until adequate separation of the organic and aqueous layers was observed. The lower organic layer only was collected carefully into fresh Teflon-capped glass tubes. The organic layer was then dried under nitrogen gas until completely dry and stored at -20°C. Immediately before mass spectrometric analysis, the lipid extracts were resuspended in 300uL of 9:1 methanol:chloroform (v/v).

### Mass Spectrometric Lipidomics

Lipid extracts were separated on a Kinetex HILIC column (150 mm x 2.1 mm, 2.6 µm: (Phenomenex, Torrance, CA, USA) connected to a Ultimate 3000 UltraHigh Performance Liquid Chromatograph

(UHPLC) with autosampler and an Exactive benchtop Orbitrap mass spectrometer (MS) (Thermo Fisher Scientific, San Jose, CA) equipped with a electrospray ionization (ESI) probe. The column oven temperature was maintained at 25°C, and the temperature of the autosampler was set to 4°C. For each analysis, 10 μL was injected onto the column. Separations ran for 35 minutes at a UHPLC flow rate of 0.2 mL/min with mobile phase A and B consisting of 10 mM aqueous ammonium formate pH 3 and 10 mM ammonium formate pH 3 in 93% (v/v) can, respectively. The gradient started at 100% B and was altered based on the following profile: $t$ = 0 minutes, 100% B; $t$ = 1 minute, 100% B; $t$ = 15 minutes, 81% B, 29% A; $t$ = 15.1 minutes, 48% B, 52% A; $t$ = 25 in, 48% B, 52% A; $t$ = 25.1 minutes, 100% B, $t$ = 35 minutes, 100% B. The same LC conditions and buffers were used for all MS experiments described below.

The MS spray voltage was set to 4 kV, and the heated capillary temperature was set at 350°C. The sheath and auxiliary gas flow rates were set to 25 units and 10 units, respectively. These conditions were held constant for both positive and negative ionization mode acquisitions, which were both performed for every sample. External mass calibration was accomplished using the standard calibration mixture and protocol from the manufacturer approximately every 2 days. For full scan profiling experiments, the MS was run with resolution of 140,000 with a scan range of 113-1700 *m/z*. For lipid identification studies, HCD fragmentation experiments were run. These experiments were performed by alternating between full scan acquisitions and all ion fragmentation HCD scans. Samples were analyzed in both positive and negative mode, and full scan settings were the same as listed above. For the all ion fragmentation scans, the resolution was 140,000 with a scan range of 113-1700 *m/z*. The normalized collision energy was 30eV, and a stepped collision energy algorithm of 50% was used. Full scan MS data was evaluated using Maven software (15), and lipid classes were identified by their fragments using the Xcalibur software package (Thermo Fisher Scientific, San Jose, CA) and information from the LIPID MAPS initiative (16). Lipid species were verified using retention times, high mass accuracy, and fragmentation data. Internal standards were not used in this study; therefore, the relative amounts of each phospholipid species are

presented. Inter-class comparisons are possible, although some approximation of the relative intensities is inherent due to differing ionization efficiencies among lipids with different acyl chain lengths.

**Phosphatidylserine Synthase Assay**

This procedure was done as described in (13,17) with minor alterations. Cultures were grown over night and then diluted into 1 L YPD, approximately 0.1 $OD_{600}$/mL. These cultures were shaken at 30°C for 6 to 10 hours. Cells were then harvested by centrifugation at 6,000 xg for 20 minutes. Pellets were then transferred to 50 mL conical tubes and washed with water and re-pelleted. Supernatant was removed and the wet weight of the samples was taken. Cell pellets were stored overnight in -80°C. The following day, a cold mixture of 0.1 M Tris-Cl pH 7.5, 5 mM β-mercaptoethanol (BME), 10% glycerol, and protease inhibitors (phenylmethylsuphonylfluoride (PMSF), leupeptin, and pepstatin) was added to the frozen pellets (1mL/g [wet weight]) and allowed to thaw on ice. Cells were lysed using a French Press (three passes at approximately 13,000 $lb/in^2$). The homogenate was centrifuged at 4°C for 5 minutes at 3,000 rpm to clear unbroken cells and heavy material. Supernatant was then spun again at 27,000 g for 10 minutes at 4°C. For some experiments, the resulting supernatant was then spun at 100,000 g to collect the lower density membranes. Pellets were resuspended in 500 µL to 1 mL of 0.1 M Tris-Cl pH 7.5, 5 mM β-mercaptoethanol (BME), 10% glycerol, and protease inhibitors. This mixture was aliquoted into microcentrifuge tubes and homogenized to break apart clumps, keeping on ice as much as possible. Total crude protein concentration was determined using a Bradford Assay. The optimal assay mixture contained 50 mM Tris-HCl pH 7.5, 0.1% Triton X-100, 0.5 mM $MnCl_2$, 0.1 mM CDP-DAG (Avanti Polar Lipids, Alabaster, AL) added as a suspension in 1% to 20% Triton X-100 and 0.4-0.5 mg protein in a total volume of 0.1 mL.

The PS synthase assay was performed by monitoring the incorporation of 0.5 mM L-serine spiked with 5% by volume [$^3$H]-L-serine (~20 Ci/mmol) into the chloroform-soluble product at 37°C for a predetermined amount of time. The reaction was terminated by the addition of 1 mL chloroform: methanol (2:1). Following a low-speed spin, 800 to 1000 µL of the supernatant was removed to a fresh tube and washed with 200 µL 0.9% NaCl. Following a second low-speed spin, 400-500 µL of the

chloroform phase was removed to a new tube and washed with 500 µL of chloroform: methanol: 0.9% NaCl (3:48:47). Following a third low-speed spin, 200-300 µL was transferred into scintillation vials (Thermo Fisher Scientific, San Jose, CA). Tubes were left open in the hood until dried fully. The next day, 2.5 mL scintillation fluid was added to each tube and run through the scintillation counter.

**Statistical analysis**

Graphs were made using GraphPad Prism version 6.04. Unpaired t-tests were used to determine significance between results. The lipidomics data were normalized by dry weight prior to statistical analyses.

**Results and Discussion**

**Phospholipids synthesized in the de novo pathway are dominated by 34:n species**

Phospholipid profiles have previously been generated for the *cho1*ΔΔ*, psd1*ΔΔ, and *psd1*ΔΔ *psd2*ΔΔ mutants using [$^{32}$P]-labeled phospholipids and thin layer chromatography (TLC) (10). However, TLC only reveals levels of different lipid classes (polar head groups). We wanted to also determine the differences among the individual species (fatty acid composition) within each class. Thus, profiles of the major phospholipid classes were generated via lipidomics from lipids extracted from wildtype, *cho1ΔΔ*, *cho1ΔΔ::CHO1*, *psd1ΔΔ*, *psd1ΔΔ::PSD1*, *psd2ΔΔ*, *psd2ΔΔ::PSD2*, *psd1ΔΔ psd2ΔΔ* strains of *C. albicans*. The lipids were analyzed by UHPLC-ESI-MS using the protocol described in methods and materials. Profiles of PI, PG, CL, PS, PE, and PC from three biological replicates were generated and are shown in Figure 2. Statistically significant differences for particular species within each class compared to wild-type are shown in Supplemental Table 1.

In the *cho1*ΔΔ mutant, which lacks PS synthase (the initial step in the *de novo* pathway, Fig. 1), PS is essentially absent, as expected (Fig. 2). The *cho1ΔΔ::CHO1* reintegrant strain exhibited a modest return of PS levels as compared with the *cho1ΔΔ* and WT strains. The reintegrant strain has only one copy of *CHO1*, so haploinsufficiency is a possible explanation of this result. However, since the level of

PS in the reintegrant is only about 37% of the wildtype, one allele may be dominant over the other. *C. albicans* has well-documented heterozygosity, which could account for this result (18).

The distribution of PS species in the WT consists predominantly of 34:n species (~88%), with 34:2 being the most prevalent (Fig 2). The *psd1*ΔΔ mutant, that lacks the dominant PS decarboxylase (predicted to be localized to the mitochondria) that converts PS to PE, exhibits an overall increase in PS, but especially of the 34:2 species. A slight increase in PS is seen in the *psd2*ΔΔ mutant, which lacks the alternative PS decarboxylase (predicted to localize to the Golgi/endosome). The reintegrant strains *psd1*ΔΔ*::PSD1* and *psd2*ΔΔ*::PSD2* also show slight increases in levels of PS. The *psd1*ΔΔ *psd2*ΔΔ mutant, which lacks all PS decarboxylase activity, has over a 3-fold increase in PS species overall, but individual species are over-represented by 2 to 5 fold. The 34:n species, which were the most abundant in WT, are also the most abundant in the *psd1*ΔΔ *psd2*ΔΔ and over-represented by ~5 fold compared to WT. However, it appears that all species are decarboxylated to some extent, given that they build up as well.

PE is the direct downstream product of PS decarboxylation (Fig. 1), and loss of PS was expected to result in a sizeable decrease in PE, but surprisingly we saw increases in PE levels in most of our mutants (Fig. 2). Most of these changes are not statistically significant in the majority of mutants, including *cho1*ΔΔ (Supplemental Table 1), although they are for *psd1*ΔΔ *psd2*ΔΔ. The maintenance of PE levels by the *cho1ΔΔ* and *psd1*ΔΔ *psd2*ΔΔ mutants is likely due to growing these cultures in YPD, a rich medium containing ethanolamine and choline. Since the *cho1ΔΔ* and *psd1*ΔΔ *psd2*ΔΔ mutants have no production of PE via the CDP-DAG pathway, it is likely that these mutants compensate through activity from the Kennedy Pathway in order to synthesize PE. The *psd1*ΔΔ mutant, which is missing the mitochondrial Psd activity, showed WT-levels of PE, suggesting that the loss of Psd1p was rescued by the redundant function of Psd2p. The *psd2*ΔΔ strain exhibited an increase in PE, but this was again not statistically significant. The *psd2*ΔΔ*::PSD2* strain did have significant increases in many phospholipids, which was unexpected. The *psd1*ΔΔ*::PSD1* did not show many significant differences from WT. Overall, the majority of PE species in WT are of 36:n (~57%) or 34:n (40%), and even in the *psd1*ΔΔ *psd2*ΔΔ

where the changes were significant, this only shifted by less than 10% compared to WT (65% 36:n and 32% 34:n).

Since the majority of PS is 34:n (~88%) in WT cells, the Kennedy Pathway may account for half of the PE population (34:n) or significant acyl remodeling of PS-derived PE is used to create other species upon or just prior to decarboxylation. However, since a similar distribution of PE is found in WT, *cho1*ΔΔ (totally lacks PS), and *psd1*ΔΔ *psd2*ΔΔ strains (cannot convert PS to PE), this suggests that most of the 36:n PE is derived from the Kennedy pathway, and the Kennedy pathway also synthesizes 34:n PE efficiently or converts 36:n by acyl remodeling.

Previous studies with *S. cerevisiae* showed an accumulation of PC in the *cho1*Δ mutant based upon TLC analysis (19). Indeed, our data show an approximately 1.5 fold increase in the level of PC in both the *cho1*ΔΔ and *psd1*ΔΔ *psd2*ΔΔ mutants when compared to the WT (Fig 2). The most obvious common relationship between *cho1*ΔΔ and *psd1*ΔΔ *psd2*ΔΔ is that both have a complete loss of *de novo* PE synthesis, which may indicate that this metabolic alteration causes an increase in PC synthesis via the Kennedy pathway. In the *psd1*ΔΔ *psd2*ΔΔ or *cho1*ΔΔ mutants, PC can be synthesized directly from choline and DAG via the Kennedy pathway or by methylation of Kennedy-pathway-derived PE via the *de novo* pathway (Fig. 1). However, from this data it is not possible to determine the level of PC coming directly from Kennedy pathway versus the methylation of Kenney pathway derived PE to PC. Interestingly, the *cho1*ΔΔ*::CHO1* strain, which has only one allele of *CHO1*, has WT levels of PC. Loss of PS decarboxylase activity in *psd1*ΔΔ or *psd2*ΔΔ mutants also has little effect on PC levels when compared with that of WT. Although there is a slight decrease in PC in the *psd2*ΔΔ mutant, it does not appear to be statistically significant. These findings suggest that the organism strictly controls the production of PC to at least maintain WT levels. The majority of PC species are 36:n and 38:n. It is possible that the 36:n PC is formed through the *de novo* methylation of 36:n PE. The 38:n species are probably produced from the importation of exogenous choline. However, there are no striking changes within lipid species across mutant strains to confirm or deny these hypotheses.

**Increases in other CDP-DAG derived phospholipids may be caused by an abundance of substrate in the PS synthase and PS decarboxylase mutants**

Phosphatidic acid (PA) is the precursor for CDP-DAG that is used to produce PS, PG, and PI (Fig. 1). The *cho1*ΔΔ mutant showed a nearly 3 fold increase in PA levels when compared to WT (Fig 2). These results were expected because the loss of PS synthesis causes a major blockage in *de novo* phospholipid synthesis, which would in turn lead to a build-up of the precursor molecule PA (substrate for CDP-DAG). This is further supported by the intermediate level of PA in *cho1*ΔΔ*::CHO1*, which correlates with the partial return of PS production, and thus increased usage of PA. Varying increases are shown in PA levels within *psd1*ΔΔ and *psd2*ΔΔ mutants and their reintegrant strains, again potentially relating back to the build-up of PS in these strains, which translates into a build-up of PA. This is supported by the large increase in PA seen in *psd1*ΔΔ *psd2*ΔΔ, which has no *de novo* PE production, and thus represents a blockage in this biosynthetic pathway.

We also aimed to analyze the levels of CDP-DAG within our mutants and found that we could only detect 32:0 species and that the overall levels of this precursor lipid were extremely low (data not shownFigure 2B). This suggests that there is a high turnover of CDP-DAG and that it is rapidly used to produce PS, PI, or PG. Although there was some variability within the CDP-DAG levels, including increases in most of the mutants tested, none of these changes were statistically significant when compared to WT. However, the change in CDP-DAG levels within our mutants again could easily be attributed to a back up in the *de novo* synthesis (either a halt of PS production or usage) which causes increases in CDP-DAG levels.

In addition to the precursors, we also looked at the levels of the other two phospholipids produced from CDP-DAG, PI and PG, as well as CL which is produced from two PG molecules. Both the *cho1*ΔΔ and the *psd1*ΔΔ *psd2*ΔΔ mutants show increases in PI and PG levels. Where the *cho1*ΔΔ PI levels increase by around 2.5 fold, the *psd1*ΔΔ *psd2*ΔΔ increase is more modest. For PG we see an increase in both *cho1*ΔΔ and *psd1*ΔΔ*psd2*ΔΔ, at approximately 5-fold and 4-fold, respectively. These findings could be a result of more CDP-DAG being available for the production of PI and PG due to a blockage of PS

synthesis (*cho1*ΔΔ) or a build-up in PS (*psd1*ΔΔ *psd2*ΔΔ). PI and PG seem to be tightly controlled, however, because in all other mutant and reintegrant strains, the levels return to WT. Finally, levels of CL correspond well with the changes in PG within our mutant strains. This indicates that some of the excess PG produced can be further modified to produce CL. These findings correlate well with studies in *S. cerevisiae* and confirm our previous results with TLC (10,19). Interestingly, as PS, the most abundant species of PI and PG appear to be 34:n, thus it is possible that most CDP-DAG destined for PS synthesis is 34:n, but our lipidomics yields of CDP-DAG were too low to verify this, and it may be 34:n CDP-DAG is so rapidly processed into other lipids that it is hard to detect at steady-state.

**Phosphatidylserine Synthesis in PS synthase and PS decarboxylase mutants**

The *psd1*ΔΔ *psd2*ΔΔ mutant exhibits a large increase in PS levels (Fig. 2), which is presumed to be caused by decreased decarboxylation of PS to PE. However, it is possible that this is due to increased PS synthase activity instead. This seemed doubtful, but to test this, an *in vitro* PS synthase assay was performed on cellular membranes, which were isolated from cell lysates via a 27,000xg centrifugation step. Additional low density membranes were isolated via a 100,000xg centrifugation step. However, as highly variable results were found in the 100,000xg membrane prep, data was generated from the 27,000xg membranes which provided more consistent results. The assay was used to compare the incorporation of [$^3$H]-serine into membranes upon the addition of CDP-DAG between WT, *cho1ΔΔ*, *cho1ΔΔ::CHO1*, *psd1ΔΔ*, *psd1ΔΔ psd2ΔΔ*, and *psd1ΔΔ::PSD1* strains. WT levels of PS synthase activity were seen in the wildtype, *psd1ΔΔ*, and *psd1ΔΔ psd2ΔΔ* strains, indicating that these strains have similar enzyme activities (Fig. 3). Thus, the excess PS in the *psd1*ΔΔ *psd2*ΔΔ mutant is likely a product of the loss of PS decarboxylase activity and build up of substrate.

As expected from this assay, the *cho1*ΔΔ mutant exhibited no PS synthase activity. However, the *cho1*ΔΔ*::CHO1* reintegrant strain had only about 10% of the activity of the wild-type. This compares with the decreased PS levels in the reintegrant as measured by lipidomics (Fig. 2). Haploinsufficiency may account for some lower activity, but as the activity is below 50%, the reconstituted allele could be

less effective. This may be because one *CHO1* allele is dominant over the other or the reintegration construct is not as efficient.

**_C. albicans_ Cho1p enzyme kinetics are similar to those reported for _S. cerevisiae_**

The WT and other strains seemed to have similar PS synthase activity levels, but it was of interest to know more about the enzyme kinetics of *C. albicans* Cho1p, if it is to be considered for potential use as a drug target. The $K_m$ and apparent $V_{max}$ of this enzyme was calculated for both serine and CDP-DAG (Fig. 4). L-serine, where the CDP-DAG was held constant at 0.1 mM, yielded a $K_m$ of 1.2±0.57 mM and an apparent $V_{max}$ of 0.15±0.02 nmole/minute/mg of protein (Fig 4A). For CDP-DAG, where the serine was held constant at 2.5 mM, a $K_m$ of 43.17±19.18 μM and an apparent $V_{max}$ of 0.19±0.023 nmole/minute/mg of protein (Fig 4B) was obtained. Interestingly, the intracellular concentration of serine in *S. cerevisiae* has been estimated to be around 2 mM on average (20), which fits well with the *Km* for serine. These assays were performed on the crude 27,000xg membranes in order to determine their kinetics within native membranes. These compare relatively closely with what has been reported for *S. cerevisiae* (13).

To control for the possibility that any similar substrate molecules to serine might give a similar activity, which could cast doubt on the accuracy of the assay, we determined whether increasing concentrations of cold D-serine or threonine (similar amino acid) could compete with [$^3$H]-L-serine for incorporation into [$^3$H]-PS. Only at the highest concentration of 200 mM (400x) did the cold D-serine show any competition with L-serine (Fig. 5). Threonine showed no statistically significant competition with L-serine, even at 200mM (400x). As a control, cold L-serine eliminated incorporation of [$^3$H]-L-serine at a 10x concentration (5 mM). Thus, this assay would not yield a product with these two similar molecules, thus suggesting that the assay is specifically measuring activity against L-serine.

**Conclusions**

The loss of *de novo* PE synthesis and/or PS synthesis has striking effects on the phospholipidome, which are consistent with what we know from fungal phospholipid metabolism. In particular, the loss of the *de*

285 *novo* pathway for PS and/or PE synthesis appears to increase the synthesis of other CDP-DAG-dependent
286 phospholipids like PI and PG (Figure 2). Surprisingly, PE and PC levels appear to be buffered against
287 change, presumably by the activity of the Kennedy pathway. The 34:n species are the most prominent
288 forms of PS, and 34:2 in particular is the most actively used substrate by Psd enzymes to synthesize PE,
289 and the 34:2 species is also what builds up in PI and PG, which may suggest that either Cho1p
290 preferentially uses 34:2 CDP-DAG, or 34:2 CDP-DAG is what it encounters in its subdomains in the ER.
291 Finally, our analysis of the enzymology of Cho1p from *C. albicans* reveals it is very similar to *C.*
292 *S. cerevisiae*, and that changes in the enzyme activity, for example in the *CHO1* compared to
293 *cho1*ΔΔ*::CHO1* strains, seem to correlate with one another rather closely. These analyses set the stage
294 for better understanding how strategies to inhibit *de novo* PS or PE synthesis, which are required for
295 virulence of *C. albicans*, may impact overall lipid profiles and ability to cause disease.
296

**Acknowledgements**

The authors would like to acknowledge Joel C. Bucci at Louisiana State University and Dr. Melinda Hauser at the University of Tennessee for their advice and guidance with enzyme kinetics experiments and calculations. We would also like to thank Dr. Jana Patton-Vogt at Duquesne University for technical assistance with the PS synthase assay.

**Grant Support**

This work was funded by the NIH R01AL105690.

## Literature Cited


1. Morrell, M., Fraser, V.J. and Kollef, M.H. (2005) Delaying the empiric treatment of candida bloodstream infection until positive blood culture results are obtained: a potential risk factor for hospital mortality. *Antimicrob Agents Chemother*, **49**, 3640-3645.
2. Wisplinghoff, H., Bischoff, T., Tallent, S.M., Seifert, H., Wenzel, R.P. and Edmond, M.B. (2004) Nosocomial bloodstream infections in US hospitals: analysis of 24,179 cases from a prospective nationwide surveillance study. *Clin Infect Dis*, **39**, 309-317.
3. Pfaller, M., Neofytos, D., Diekema, D., Azie, N., Meier-Kriesche, H.U., Quan, S.P. and Horn, D. (2012) Epidemiology and outcomes of candidemia in 3648 patients: data from the Prospective Antifungal Therapy (PATH Alliance(R)) registry, 2004-2008. *Diagn Microbiol Infect Dis*, **74**, 323-331.
4. Mishra, N.N., Prasad, T., Sharma, N., Payasi, A., Prasad, R., Gupta, D.K. and Singh, R. (2007) Pathogenicity and drug resistance in Candida albicans and other yeast species. A review. *Acta Microbiol Immunol Hung*, **54**, 201-235.
5. Ghannoum, M.A. and Rice, L.B. (1999) Antifungal agents: mode of action, mechanisms of resistance, and correlation of these mechanisms with bacterial resistance. *Clin Microbiol Rev*, **12**, 501-517.
6. Holeman, C.W., Jr. and Einstein, H. (1963) The toxic effects of amphotericin B in man. *Calif Med*, **99**, 90-93.
7. Low, C.Y. and Rotstein, C. (2011) Emerging fungal infections in immunocompromised patients. *F1000 Med Rep*, **3**, 14.
8. Singh, A., Yadav, V. and Prasad, R. (2012) Comparative lipidomics in clinical isolates of Candida albicans reveal crosstalk between mitochondria, cell wall integrity and azole resistance. *PLoS One*, **7**, e39812.
9. Henry, S.A., Kohlwein, S.D. and Carman, G.M. (2012) Metabolism and regulation of glycerolipids in the yeast Saccharomyces cerevisiae. *Genetics*, **190**, 317-349.
10. Chen, Y.L., Montedonico, A.E., Kauffman, S., Dunlap, J.R., Menn, F.M. and Reynolds, T.B. (2010) Phosphatidylserine synthase and phosphatidylserine decarboxylase are essential for cell wall integrity and virulence in Candida albicans. *Mol Microbiol*, **75**, 1112-1132.
11. Gibellini, F. and Smith, T.K. (2010) The Kennedy pathway--De novo synthesis of phosphatidylethanolamine and phosphatidylcholine. *IUBMB Life*, **62**, 414-428.
12. Braun, B.R., van Het Hoog, M., d'Enfert, C., Martchenko, M., Dungan, J., Kuo, A., Inglis, D.O., Uhl, M.A., Hogues, H., Berriman, M. *et al.* (2005) A human-curated annotation of the Candida albicans genome. *PLoS Genet*, **1**, 36-57.
13. Bae-Lee, M.S. and Carman, G.M. (1984) Phosphatidylserine synthesis in Saccharomyces cerevisiae. Purification and characterization of membrane-associated phosphatidylserine synthase. *J Biol Chem*, **259**, 10857-10862.
14. Singh, A., Prasad, T., Kapoor, K., Mandal, A., Roth, M., Welti, R. and Prasad, R. (2010) Phospholipidome of Candida: Each Species of Candida Has Distinctive Phospholipid Molecular Species. *Omics*, **14**, 665-677.
15. Melamud, E., Vastag, L. and Rabinowitz, J.D. (2010) Metabolomic analysis and visualization engine for LC-MS data. *Anal Chem*, **82**, 9818-9826.
16. Fahy, E., Sud, M., Cotter, D. and Subramaniam, S. (2007) LIPID MAPS online tools for lipid research. *Nucleic Acids Res*, **35**, W606-612.

17. Matsuo, Y., Fisher, E., Patton-Vogt, J. and Marcus, S. (2007) Functional characterization of the fission yeast phosphatidylserine synthase gene, pps1, reveals novel cellular functions for phosphatidylserine. *Eukaryot Cell*, **6**, 2092-2101.
18. Eckert, S.E. and Muhlschlegel, F.A. (2009) Promoter regulation in Candida albicans and related species. *FEMS Yeast Res*, **9**, 2-15.
19. Atkinson, K., Fogel, S. and Henry, S.A. (1980) Yeast mutant defective in phosphatidylserine synthesis. *J Biol Chem*, **255**, 6653-6661.
20. Hans, M.A., Heinzle, E. and Wittmann, C. (2003) Free intracellular amino acid pools during autonomous oscillations in Saccharomyces cerevisiae. *Biotechnol Bioeng*, **82**, 143-151.

364 **Figure Legends**

365 **Figure 1: Phospholipid Biosynthesis Pathways in *C. albicans***

366 *C. albicans* phospholipid biosynthesis occurs via both an endogenous pathway, the *de novo* pathway, and
367 an exogenous pathway, the Kennedy pathway. The precursors for producing the most common
368 phospholipids are PA and CDP-DAG. CDP-DAG is then converted to PI, PS, or PG. The endogenously
369 produced PS can then be decarboxylated via Psd1/2 into PE and then further methylated into PC. In the
370 Kennedy pathway, exogenous Etn and/or Cho are brought into the cell and converted into PE and PC.
371 Abbreviations: PA – phosphatidic acid; CDP-DAG – cytidine diphosphate-diacylglycerol; PI –
372 phosphatidylinositol; PS – phosphatidylserine; PG – phosphatidylglycerol; PE –
373 phosphatidylethanolamine; CL – cardiolipin; PC – phosphatidylcholine; Etn – ethanolamine; Cho –
374 choline

375

376 **Figure 2. The phospholipid species profiles for the major classes of phospholipids in *C. albicans***
377 **phospholipid synthesis mutants**

378 **A.** The phospholipid species profiles are shown for the major phospholipid classes of phosphatidylserine
379 (PS), phosphatidylethanolamine (PE), phosphatidylcholine (PC), phosphatidylglycerol (PG),
380 phosphatidylinositol (PI) and cardiolipin (CL). **B.** The species profiles detected are shown for the
381 precursor lipids phosphatidic acid (PA) and cytidyldiphosphate-diacylglycerol (CDP-DAG). For each
382 lipid class, a stacked bar graph is used and the species associated with each color is shown in the legend
383 based on the combined carbon content and number of unsaturated bonds within the fatty acid component
384 of the phospholipid. The Y-axis of the graph is the area under the peak for each species based on spectral
385 profiles. The X-axis is the strains, which are as follows: wild-type (WT), cho1 (*cho1*ΔΔ), psd1 (*psd1*ΔΔ),
386 psd1,2 (*psd1*ΔΔ *psd2*ΔΔ), psd2 (*psd2*ΔΔ), psd2R (*psd2*ΔΔ*::PSD2*), psd1R (*psd1*ΔΔ*::PSD1*).

387

388

389

**Figure 3. Phosphatidylserine Synthase Activity Across Strains**

Cho1p activity within different mutant strains of *C. albicans*. ER membranes containing Cho1p were isolated and treated with CDP-DAG and [$^3$H]-serine. Activity is measured as counts per minute per milligram of protein. Values are shown as an average of 3 experiments averaged and normalized to the wild-type control. $P < 0.0001$

**Figure 4. Enzyme Kinetics for Cho1p**

The PS synthase assay was performed with varying concentrations of substrate over time courses to generate enzyme kinetics for both substrates. A) The Michaelis-Menton curve for the L-serine substrate shows a $K_m$ of 1.243±0.5715 mM and a $V_{max}$ of 0.1514±0.02059 nmole/minute/mg of protein. B) The Michaelis-Menton curve for the CDP-DAG substrate shows a $K_m$ of 43.17±19.18 μM and a $V_{max}$ of 0.1919±0.02361 nmole/minute/mg of protein.

**Figure 5: Cho1p shows specificity for L-serine**

PS synthase assay was performed with 0.5 mM [$^3$H]-serine and 0.1 mM CDP-DAG. An excess of D-serine (A) or L-threonine (B) was added at varying concentrations. Only D-serine or L-threonine at concentrations 400-fold that of L-serine show any inhibition in [$^3$H]-PS production. Values are shown as an average of 3 experiments averaged and normalized to the wild-type control. $P = 0.0361$

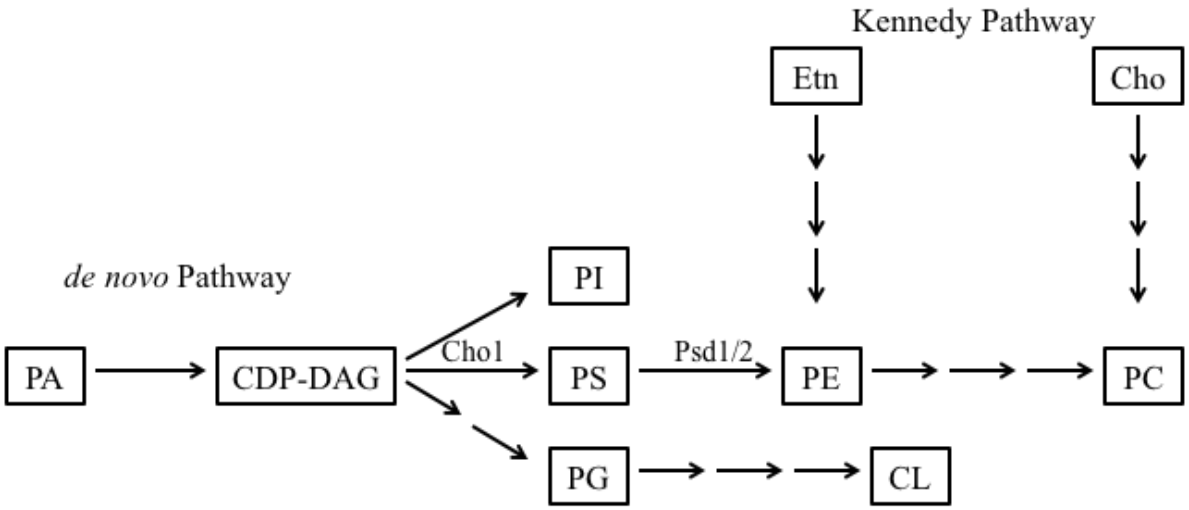


**Figure 1: Phospholipid Biosynthesis Pathways in *C. albicans***

*C. albicans* acquires phospholipids via both an endogenous pathway, the *de novo* pathway, and an exogenous pathway, the Kennedy pathway. The precursors for producing the most common phospholipids are PA and CDP-DAG. CDP-DAG is then converted to PI, PS, or PG. The endogenously produced PS can be decarboxylated into PE and then further methylated into PC. In the Kennedy pathway, exogenous ethanolamine (Etn) and/or choline (Cho) are brought into the cell and converted into PE and PC. Abbreviations: PA – phosphatidic acid; CDP-DAG – cytidine diphosphate diacylglycerol; PI – phosphatidylinositol; PS – phosphatidylserine; PG – phosphatidylglycerol; PE – phosphatidylethanolamine; CL – cardiolipin; PC – phosphatidylcholine; Etn – ethanolamine; Cho - choline

410

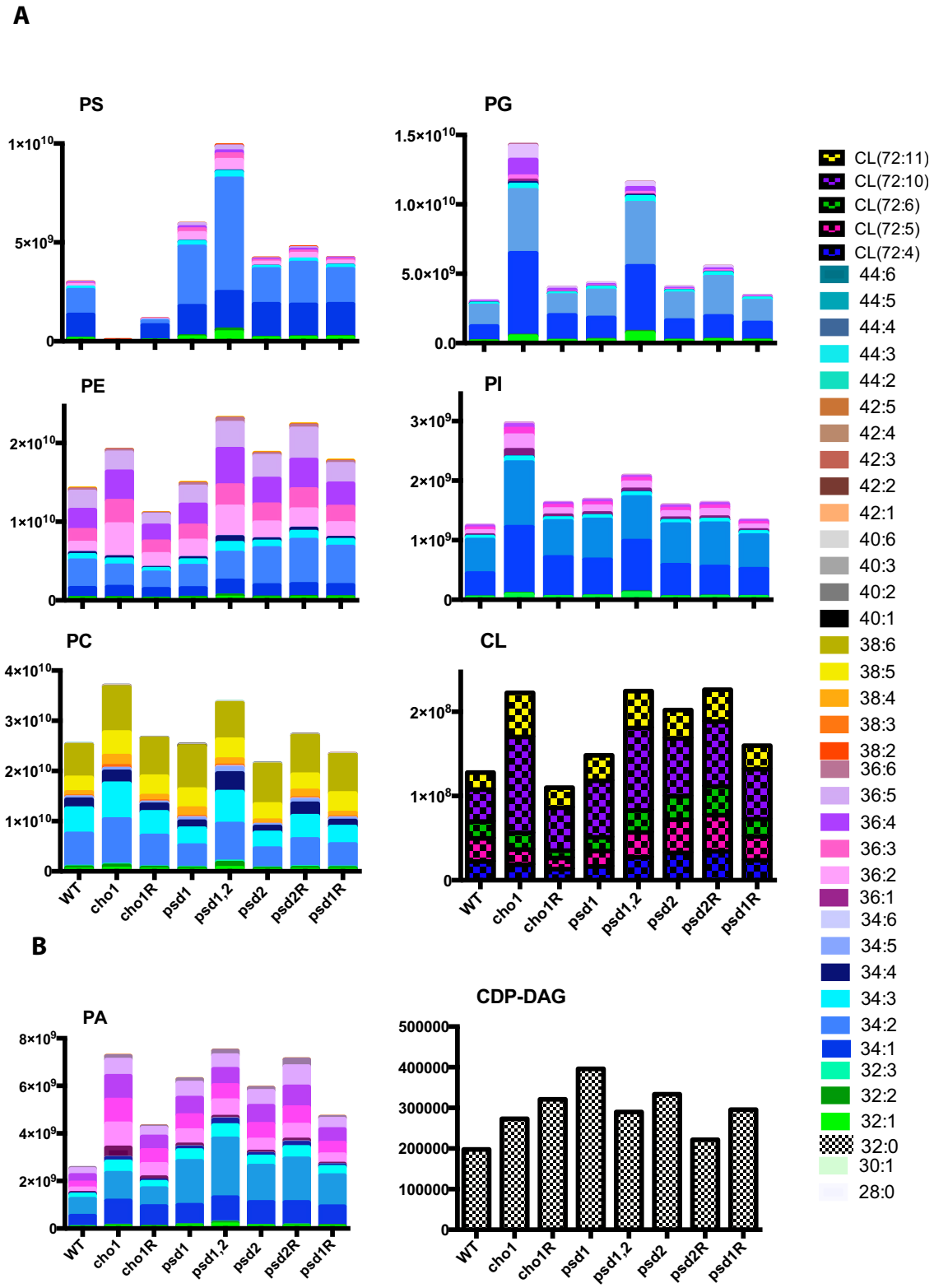
A
PS
PG
PE
PI
PC
CL
B
PA
CDP-DAG
WT
cho1
cho1R
psd1
psd1,2
psd2
psd2R
psd1R
CL(72:11)
CL(72:10)
CL(72:6)
CL(72:5)
CL(72:4)
44:6
44:5
44:4
44:3
44:2
42:5
42:4
42:3
42:2
42:1
40:6
40:3
40:2
40:1
38:6
38:5
38:4
38:3
38:2
36:6
36:5
36:4
36:3
36:2
36:1
34:6
34:5
34:4
34:3
34:2
34:1
32:3
32:2
32:1
32:0
30:1
28:0

411

412

Figure 3.

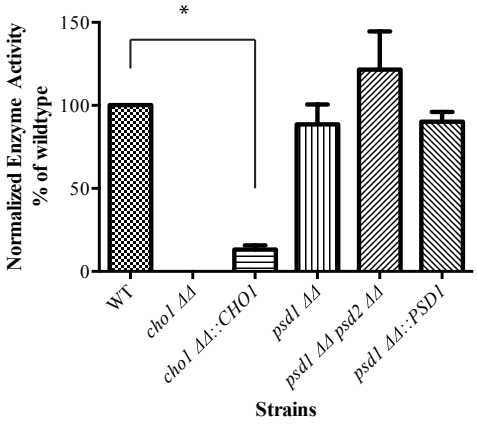


413

414

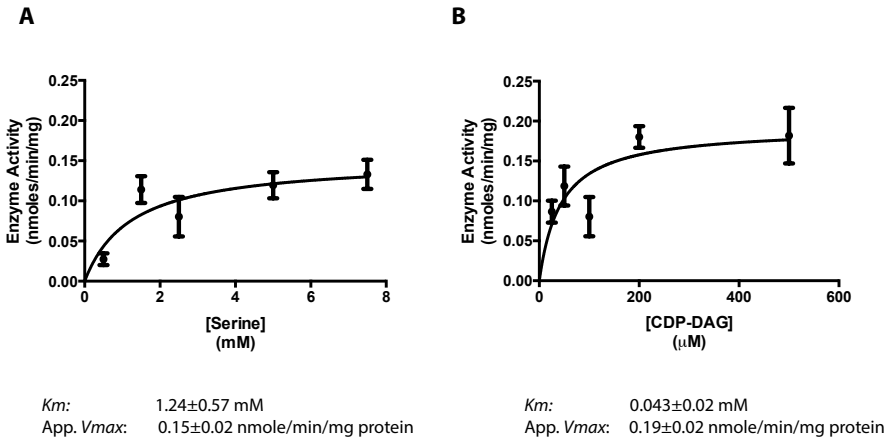


*Km:* 1.24±0.57 mM
App. *Vmax*: 0.15±0.02 nmole/min/mg protein

*Km:* 0.043±0.02 mM
App. *Vmax*: 0.19±0.02 nmole/min/mg protein

415

416

Figure 5.

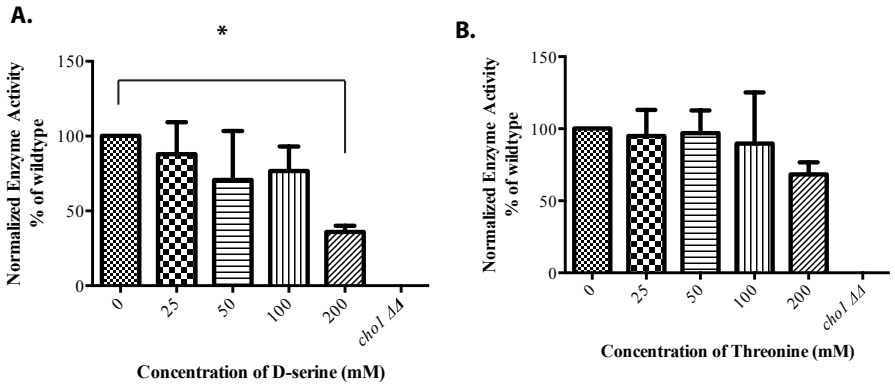


417

418

419

**STATISTICAL ANALYSES OF DIFFERENCES BETWEEN CLASSES OF LIPIDS FOR DIFFERENT STRA**

All P values are relative to wild-type: **P value <0.01 , *P value <0.05, - is not significantly d

| **Phosphatidylserine (PS)** | | | | | |
|---|---|---|---|---|---|
| | cho1 | cho1R | psd1 | psd1,2 | psd2 |
| PS(28:0) | ** | ** | ** | ** | ** |
| PS(30:1) | ** | ** | - | ** | - |
| PS(32:1) | ** | ** | ** | ** | - |
| PS(32:2) | ** | ** | ** | ** | - |
| PS(34:1) | ** | * | - | * | * |
| PS(34:2) | ** | ** | ** | ** | - |
| PS(34:3) | ** | ** | ** | ** | - |
| PS(34:4) | ** | ** | ** | ** | - |
| PS(34:5) | * | * | ** | ** | - |
| PS(36:2) | ** | ** | ** | ** | ** |
| PS(36:3) | ** | ** | ** | ** | * |
| PS(36:4) | ** | ** | ** | ** | * |
| PS(36:5) | ** | ** | ** | ** | - |
| PS(36:6) | ** | ** | ** | ** | - |
| PS(38:1) | ** | - | - | * | - |
| PS(38:2) | ** | - | - | * | - |
| PS(38:3) | * | - | - | * | - |

| **Phosphatidylethanolamine (PE)** | | | | | |
|---|---|---|---|---|---|
| | cho1 | cho1R | psd1 | psd1,2 | psd2 |
| PE(32:1) | - | - | - | ** | - |
| PE(32:2) | - | * | - | ** | - |
| PE(32:3) | - | ** | - | ** | - |
| PE(34:1) | - | - | - | ** | - |
| PE(34:2) | - | * | - | - | - |
| PE(34:3) | - | - | - | ** | - |
| PE(34:4) | - | - | - | ** | - |
| PE(34:5) | - | ** | - | ** | - |
| PE(36:2) | * | * | - | ** | ** |
| PE(36:3) | * | - | - | ** | * |
| PE(36:4) | - | - | - | ** | - |
| PE(36:5) | - | - | - | * | - |
| PE(36:6) | - | - | - | ** | - |
| PE(38:3) | * | * | - | - | - |
| PE(38:4) | ** | * | - | - | - |
| PE(38:5) | ** | ** | - | * | - |

| **Phosphatidylcholine (PC)** | | | | | |
|---|---|---|---|---|---|
| | cho1 | cho1R | psd1 | psd1,2 | psd2 |

420